# Astrophysical S-factor for the $^3$He$(\alpha, \gamma)^7$Be reaction via the asymptotic normalization coefficient (ANC) method

G. G. Kiss[a], M. La Cognata[b], C. Spitaleri[b,c], R. Yarmukhamedov[d], I. Wiedenhöver[e],
L. T. Baby[e], S. Cherubini[b,c], G. D'Agata[b,c,f], A. Cvetinović[b], P. Figuera[b], G. L. Guardo[b,c],
M. Gulino[b,g], S. Hayakawa[b,h], I. Indelicato[b,c], L. Lamia[b,c,i], M. Lattuada[b,c], F. Mudò[b,c],
S. Palmerini[j,k], R. G. Pizzone[b], G. G. Rapisarda[b,c], S. Romano[b,c,i], M. L. Sergi[b,c],
R. Spartà[b,c], O. Trippella[j,k], A. Tumino[b,g], M. Anastasiou[e], S.A. Kuvin[e], N. Rijal[e], B.
Schmidt[e], S. B. Igamov[d], S. B. Sakuta[l], K. I. Tursunmakhatov[d,m], Zs. Fülöp[a], Gy. Gyürky[a],
T. Szücs[a], Z. Halász[a], E. Somorjai[a], Z. Hons[f], J. Mrázek[f], R. E. Tribble[n],
A. M. Mukhamedzhanov[n]

[a]Institute for Nuclear Research (ATOMKI), H-4001 Debrecen, POB.51, Hungary
[b]Istituto Nazionale di Fisica Nucleare, Laboratori Nazionali del Sud, 95123 Catania, Italy
[c]Dipartimento di Fisica e Astronomia "E. Majorana", Università di Catania, 95123 Catania, Italy
[d]Institute of Nuclear Physics, Uzbekistan Academy of Sciences, 100214 Tashkent, Uzbekistan
[e]Department of Physics, Florida State University, Tallahassee, Florida 32306, USA
[f]Nuclear Physics Institute of the Czech Academy of Sciences, 250 68 Řež, Czech Republic
[g]Facoltà di Ingegneria e Architettura, Università di Enna "Kore", 94100, Enna, Italy
[h]Center for Nuclear Study (CNS), University of Tokyo, RIKEN campus, Saitama 351-0198, Japan
[i]Centro Siciliano di Fisica Nucleare e Struttura della Materia (CSFNSM), Catania 77843, Italy
[j]Dipartimento di Fisica e Geologia, Università di Perugia, 06123 Perugia, Italy
[k]Istituto Nazionale di Fisica Nucleare, Sezione di Perugia, Perugia, Italy
[l]National Research Center "Kurchatov Institute", Moscow 123182, Russia
[m]University of Gulistan, Gulistan, Uzbekistan
[n]Cyclotron Institute, Texas A&M University, College Station, Texas 77843, USA

## Abstract

The detection of the neutrinos produced in the $p - p$ chain and in the CNO cycle can be used to test the Standard Solar Model. The $^3$He$(\alpha, \gamma)^7$Be reaction is the first reaction of the $2^{nd}$ and $3^{rd}$ branch of the $p - p$ chain, therefore, the uncertainty of its cross section sensitively influences the prediction of the $^7$Be and $^8$B neutrino fluxes. Despite its importance and the large number of experimental and theoretical works devoted to this reaction, the knowledge on the reaction cross section at energies characterizing the core of the Sun (15 keV - 30 keV) is limited and further experimental efforts are needed to reach the desired ($\approx 3\%$) accuracy. The precise knowledge on the external capture contribution to the $^3$He$(\alpha, \gamma)^7$Be reaction cross section is crucial for the theoretical description of the reaction mechanism. In the present work the indirect measurement of this external capture contribution using the Asymptotic Normalization Coefficient (ANC) technique is reported. To extract the ANC, the angular distributions of deuterons emitted in the $^6$Li$(^3$He$,d)^7$Be $\alpha$-transfer reaction were measured with high precision at $E_{^3He} = 3.0$ MeV and $E_{^3He} = 5.0$ MeV. The ANCs were then extracted from comparison of DWBA calculations to the measured data and the zero energy astrophysical $S$-factor for $^3$He$(\alpha, \gamma)^7$Be reaction was found to be 0.534 ± 0.025 keVb.

*Keywords:* Nuclear astrophysics, Nucleosynthesis
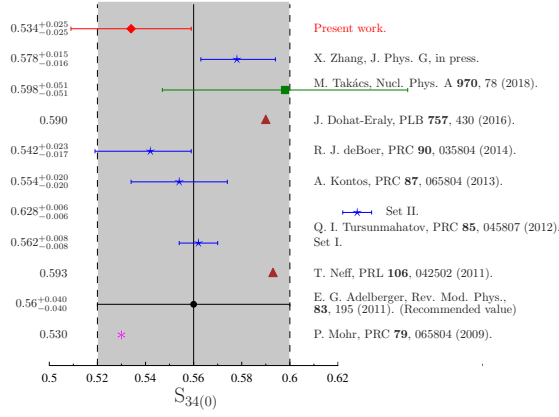
Figure 1. Summary of the most recent $^3$He$(\alpha,\gamma)^7$Be $S_{34}(0)$ factor results: derived from the analysis of elastic scattering angular distributions [23] (pink star), theoretical calculations [26, 31] (dark red triangle), extrapolations of experimental data sets [14, 24, 29, 32] (blue star), prediction based on neutrino yield measurement [57] (green box) and derived using the ANC technique (present work, red diamond) The solid central line represents the recommended value of [2], with its uncertainty indicated with the shaded area. For Tursunmahatov et al. [24], the $S_{34}(0)$ value obtained by fitting [11, 13, 15, 16] is shown.

## 1. Introduction

The $^3$He$(\alpha,\gamma)^7$Be is one of the key reactions in nuclear astrophysics, which remained critical after decades, despite the large number of experimental and theoretical studies devoted to it. This is predominantly due to the fact that the astrophysically relevant energy region, the so-called Gamow window, lies between about 15 keV and 30 keV for a temperature of 15 MK, characterizing the core of the Sun, and at these temperatures the $^3$He$(\alpha,\gamma)^7$Be reaction cross section is far too small to be measured directly. Theory-based extrapolations are therefore necessary to obtain the reaction rate [1, 2, 3]. The reaction is also important for understanding the lithium problem of the Big Bang Nucleosynthesis, at energies around 100 keV (see [4] and references therein).

The detection of the neutrinos coming directly from the core of the Sun became more and more precise after the construction of larger and more efficient neutrino detectors, sensitive to a wider neutrino energy range around the turn of the century. These neutrinos are released in the $\beta$ decay of the $^7$Be, $^8$B, $^{13}$N, $^{15}$O isotopes

produced in the $p - p$ chain and in the CNO cycle. Recently, the flux of the $p - p$ neutrinos was measured with a precision of about 3.4% by the BOREXINO, SNO and Super-Kamiokande collaborations [5, 6, 7]. The precise neutrino flux measurements can constrain the Standard Solar Model (SSM) and provide information on the core temperature of the Sun if the relevant nuclear reaction cross sections are known with matching accuracy. However, at present the uncertainties of these input parameters are far too high, typically of the order of 5-8% [8] (or even higher, see below) contrary to the 3% precision required [9, 10].

The $^3$He$(\alpha,\gamma)^7$Be reaction is the first reaction of the $2^{nd}$ and $3^{rd}$ $p - p$ chain branch and therefore the uncertainty of its rate strongly influences the precision of the predicted flux of the aforementioned $^7$Be, $^8$B neutrinos. Thus, an improvement on the knowledge of the low-energy cross section of this reaction would result in a substantial reduction of the uncertainties of the solar neutrino flux and might have important consequences for the SSM.

Not surprisingly the $^3$He$(\alpha,\gamma)^7$Be is among those reactions which were the most intensively studied in the past and the results were extensively discussed in review papers [1, 2, 3] (and references therein). Because of insufficient experimental information to assess their systematic errors, in the most recent compilations only data collected after 2004 are taken into account [2, 3]. The experimental methods used in the "modern" studies can be sorted into three groups: the detection of prompt $\gamma$ rays [11, 12, 13, 14], the measurement of the $^7$Be activity [15, 16, 17, 18, 19], and the counting of the $^7$Be recoils with a recoil mass separator [20]. Regarding the theoretical description, several different models - including external capture models (e.g. [21]), potential models (e.g. [22, 23]), modified two-body potential approach [24], resonating group calculation (e.g. [25]), *ab initio* models (e.g. [26, 27]) and R-matrix theory [28, 29] - were used to describe the reaction.

The recommended zero energy astrophysical $S$-factor value of [2], derived using the microscopic calculations of [27, 30] and rescaled to fit the data at $E \leq 1$ MeV is $S_{34}(0) = 0.56 \pm 0.02$ (exp) $\pm 0.02$ (theory) keV b. The same experimental data set was fitted using the modified two-body potential approach and significantly larger $S_{34}(0) = 0.613^{+0.026}_{-0.063}$ keV b factor was found [24]. Excluding data set II [12, 20] would lead to $S_{34}(0) = 0.562 \pm 0.008$ keV b (see [24] for more details), which is the value shown in Fig. 1. The comprehensive R-matrix extrapolation [29], including not only the data fitted in [2] and [24] but also the recently measured higher energy cross sections [14, 17, 18], resulted in an $S_{34}(0)$

Email addresses: ggkiss@atomki.mta.hu (G. G. Kiss), lacognata@lns.infn.it (M. La Cognata), rakhim@inp.uz (R. Yarmukhamedov)

value (0.542 ± 0.011 (Monte Carlo fit) ± 0.006 (model) $^{+0.019}_{-0.011}$ (phase shift) keV b) 3.2% lower than the one recommended in [2]. Furthermore, *ab initio* no-core shell model with continuum approach was used to predict $S_{34}(0)$ and a value ($S_{34}(0)$ = 0.59 keV b) 5.3% larger than the one of [2] was found [31], almost the same as predicted by [26] ($S_{34}(0)$ = 0.593 keV b). Finally, recently effective field theory was also used to perform extrapolation and a value ($S_{34}(0)$ = 0.578 keV b) 3.2% larger than the one of [2] was found [32].

While the precision of the extrapolations are of the order of 6-7%, the difference between the $S_{34}(0)$ values exceeds 10%. The predicted $S_{34}(0)$ factors are shown Fig. 1. It is clear that the calculated $S_{34}(0)$ factors depend strongly on the model used in the extrapolations and high precision experimental data is needed to constrain the theoretical models.

Here we present the results of a new approach, proposed by A. M. Mukhamedzhanov, where the $S_{34}(0)$ factor of the $^3$He($\alpha,\gamma$)$^7$Be reaction was derived without extrapolation, using the asymptotic normalization coefficient (ANC) technique [33]. Namely, since the $^3$He($\alpha,\gamma$)$^7$Be reaction at stellar energies is a pure external direct capture process [2], it essentially proceeds through the tail of the nuclear overlap function. Therefore, the shape of the overlap function in the tail region is determined by the Coulomb interaction, thus the amplitude of the overlap function determines the rate of the capture reaction [34, 35]. Since the direct capture cross sections are proportional to the squares of the ANCs - which are found from transfer reactions - with the study of the near barrier $^6$Li($^3$He,$d$)$^7$Be $\alpha$ particle transfer reaction the ANCs for the $^3$He($\alpha,\gamma$)$^7$Be reaction can be obtained. This independent experimental approach, improving gradually our understanding on the low energy behavior of this reaction, was up-to-now never used to study the $^3$He($\alpha,\gamma$)$^7$Be reaction. Furthermore, the ANC values are also needed for the R-matrix calculations. In [29] these values were deduced from experimental cross sections and found to be between 3-5.5 fm$^{-1}$. Accordingly, the independent determination of the ANC values also increases the precision of the R-matrix extrapolations.

## 2. Experimental technique

The angular distributions of the deuterons emitted in the $^6$Li($^3$He,$d$)$^7$Be reaction were measured in two experiments performed using the 3.1 MV single ended coaxial singletron accelerator of the Department of Physics and Astronomy (DFA) of the University of Catania and
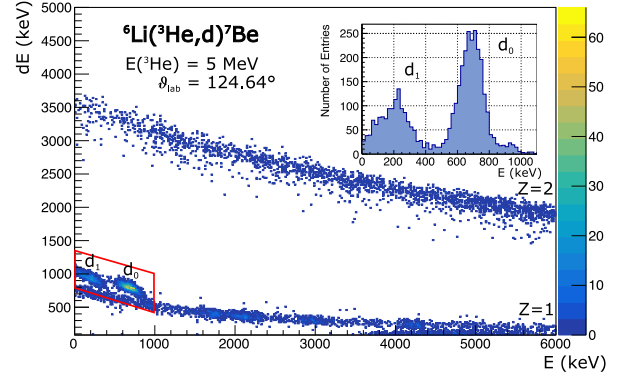
Figure 2. $\Delta E - E$ spectrum measured with a silicon telescope positioned at $\vartheta_{lab}$ = 124.64° at $E_{lab}$ = 5 MeV beam energy. The peaks (marked with $d_0$ and $d_1$) used for the analysis are indicated. The inset shows the deuteron spectrum deduced from this identification plot. Integration is performed using Gaussian fitting to remove threshold problems. The red box is used to highlight the region of interest only.

the FN tandem accelerator at the John. D. Fox Superconducting Accelerator Laboratory at the Florida State University (FSU), Tallahassee, USA. The energy of the $^3$He beam was $E_{Lab}$ = 3 MeV and $E_{Lab}$ = 5 MeV, with beam currents typically between 20 enA and 30 enA, respectively. The setup in both experiments consisted of several $\Delta E - E$ telescopes, placed on rotatable turntables and a monitor detector fixed at 165° (DFA) and 150° (FSU) with respect to the beam direction. The thicknesses of the $\Delta E$ detectors were between 8 $\mu m$ and 16 $\mu m$ and the thicknesses of the E detectors were 500 $\mu m$. In the experiment performed at DFA a 99% compound purity, 134 $\mu g$/cm$^2$ thick $^6$LiF target (enriched in 95% of $^6$Li) was used. In the experiment performed at FSU the 99% compound purity, 57 $\mu g$/cm$^2$ thick lithium target (enriched in 98% of $^6$Li) was prepared on a Formvar backing and transferred to the scattering chamber in a sealed container under vacuum to prevent oxidation. Furthermore, as it will be discussed in the following in this experiment two additional detectors were used to monitor the target thickness and for absolute normalization. In the two experiments, the yield of the emitted deuterons were measured between 23.0° $\leq \vartheta_{c.m.} \leq$ 172.5° at $E_{Lab}$ = 3 MeV and 23.2° $\leq \vartheta_{c.m.} \leq$ 168.5° at $E_{Lab}$ = 5 MeV, using typically 6° - 10° steps.

In both experiments the particle identification was performed using the standard $\Delta E - E$ technique and the peak areas - corresponding to the $^7$Be ground and 1$^{st}$ excited state - were derived by fitting Gaussian functions. An example of the two-dimensional particle identification plots is shown in Fig. 2, and the one dimensional deuteron spectrum is presented in its inset (the

peaks corresponding to the $^7$Be ground and $1^{st}$ excited state are marked with $d_0$ and $d_1$, respectively). It can be seen that the separation of the different isotopes is sufficient for reliable identification. The same procedure was used for absolute normalization in the two measurements. Namely, at first the solid angles of the detectors were derived from the known geometry and were cross-checked using radioactive sources with known activity. Furthermore, the cross section as a function of the angle of the outgoing particle in the $^6$Li($^3$He,$p$) reaction ($Q$ = 16.79 MeV) is well known [36], thus the rate of the high energy protons was measured using the monitor detector placed at a fixed position at backward angle to reconstruct the number of impinging $^3$He particles and the target thickness. At the experiment performed at FSU two further normalization techniques were used. Following the approach of [35] the yield of the $^3$He induced reactions and elastic $^3$He scattering on $^6$Li were measured with the forward monitor detectors (M1 and M2). Moreover, by placing each telescope at 95° with respect to the beam axis and measuring the $^6$Li($p$, $p$)$^6$Li elastic scattering, the target thickness and the telescope solid angles could be determined, since the $^6$Li($p$, $p$) elastic scattering cross section at 95° with $E_p$ = 6.868 MeV proton beam was previously measured with a 3% precision [37]. This approach was used in the previous experiments performed at FSU, see e.g. [38, 39]. As a result, the uncertainty of the absolute normalization was found to be 5.7% which contains uncertainties from the target thickness determination, the current measurement and the solid angle determination. Experimental angular distributions are shown in Fig. 3.

## 3. Data analysis and extraction of the ANC for the $\alpha + {}^3$He → $^7$Be system

The theoretical analysis of the data was carried out in the framework of the modified Distorted Wave Born Approximation (DWBA) [40] assuming one step proton and $\alpha$ particle transfer [41].

Accordingly — assuming $^3$He = $(d + p)$, $^7$Be = $(^6$Li + $p)$, $^6$Li = $(d + \alpha)$ and $^7$Be = $(^3$He + $\alpha)$ — for fixed values of $l_{dp}$, $j_{dp}$, $l_{d\alpha}$ and $j_{d\alpha}$, the differential cross section (DCS) for the peripheral transfer of an "$e$-particle" (where $e$ stands for $p$ or $\alpha$) in the $^6$Li($^3$He, $d$)$^7$Be reaction can be written in the form:

$$\frac{d\sigma}{d\Omega} = \sum_{j_{Ae}} C^2_{Ae;\,j_{Ae}} R^{(\text{DWBA})}_{e;\,j_{Ae}}(E_i, \theta;\, b_{ye;\,j_{ye}}, b_{Ae;\,j_{Ae}}), \quad (1)$$

$$R^{(\text{DWBA})}_{e;\,j_{Ae}}(E_i, \theta;\, b_{ye;\,j_{ye}}, b_{Ae;\,j_{Ae}}) =$$
$$C^2_{ye;\,j_{ye}} \frac{\sigma^{(\text{DWBA})}_{e;\,j_{Ae}}(E_i, \theta;\, b_{ye;\,j_{ye}}, b_{Ae;\,j_{Ae}})}{b^2_{ye;\,j_{ye}}\, b^2_{Ae;\,j_{Ae}}}, \quad (2)$$

where $B$= $A+e$ and $x$= $y+e$; $\sigma^{(\text{DWBA})}_{e;\,j_{Ae}}$ is the single-particle DWBA cross section [42], $l_{Ae}$ and $j_{Ae}$ are the orbital and total angular momenta of the transferred particles, $C's$ are the ANCs for $A + e \rightarrow B$ and $y + e \rightarrow x$, which determine the amplitudes of the tails of the radial $B$ and $x$ nucleus wave functions in the $(A + e)$ and $(y + e)$ channels [43]; $b's$ are the single-particle ANCs for the shell-model wave functions for the two-body $[B = (A+e)$ and $x = (y + e)]$ bound states, which determine the amplitudes of their tails; $E_i$ is the relative kinetic energy of the colliding particles and $\theta$ is the center-of-mass scattering angle. The negligible contribution of $d$-waves ($l_{dp} = 2$ and $l_{d\alpha} = 2$) is ignored owning to their smallness [43, 44].

Eqs. (1) and (2) are used separately for the one step $\alpha$ particle exchange reaction and for proton transfer reaction (the latter results will be published elsewhere). The $s$ wave ANC values for the $d + p \rightarrow {}^3$He and the $d + \alpha \rightarrow {}^6$Li are 4.20±0.32 fm$^{-1}$ [45] and 5.43±0.37 fm$^{-1}$ [46], respectively. According to [40, 47], the values of three parameters $b_{dp;\,j_{dp}}$ for $l_{dp} = 0$ and $j_{dp} = 1/2$ as well as of $b_{d\alpha;\,j_{d\alpha}}$ for $l_{d\alpha} = 0$ and $j_{d\alpha} = 0$ were fixed by reproducing the corresponding ANC values entering the $R^{(\text{DWBA})}_{e;\,j_{Ae}}(E_i, \theta;\, b_{ye;\,j_{ye}}, b_{Ae;\,j_{Ae}})$ function calculated separately for the one step proton transfer and $\alpha$ particle exchange mechanisms.

At the backward hemisphere the experimental differential cross section increases with increasing angles and this finding confirms the presence of a dominant one-step $\alpha$-particle exchange mechanism. Similarly, the one-step proton transfer is dominant in the forwards hemisphere. Thus, the interference of the two mechanisms at small (forward) and large (backward) angles is negligible. Accordingly, the ANCs for $^3$He + $\alpha \rightarrow {}^7$Be and for $^6$Li + $p \rightarrow {}^7$Be were extracted separately within the post form of the modified DWBA [40] using the LOLA code [42].

First, eight sets of optical potentials, obtained from the global parameter sets of [48, 49], in the input and output channels were tested and the one, providing the best description for the experimental data, was used for the further analysis. Then, the geometrical parameters $r_0$ and $a$ of the Woods-Saxon potential (having the Thomas spin-orbit term) of the two-body $^7$Be [($^6$Li + $p$) or ($^3$He + $\alpha$)] bound state wave function were varied in

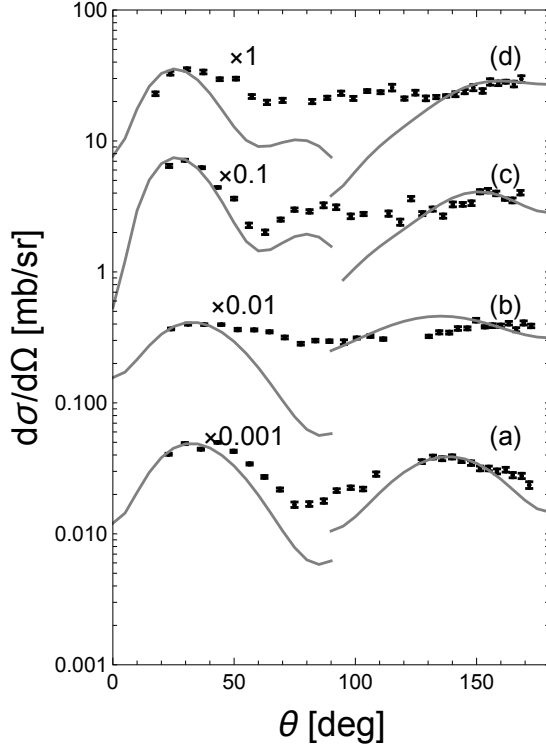tions for each experimental point of $\theta^{exp}$ – belonging to the backward and forward peak regions – were determined using the FRESCO code [51] by taking into account only one step processes with proton stripping $^6$Li($^3$He, $d$)$^7$Be and exchange mechanism with the $\alpha$-particle cluster transfer $^6$Li($^3$He, $^7$Be)$d$. The nine nucleons, present in the entrance channel, were replaced by three subsystems: i) $^3$He + $^6$Li(g.s., $J^\pi$= 1$^+$; $E^*$= 2.185 MeV, $J^\pi$= 3$^+$); ii) $d$ + $^7$Be(g.s., $J^\pi$ = 3/2$^-$; $E^*$= 0.429 MeV, $J^\pi$= 1/2$^-$) — $p$−transfer — and iii) $^7$Be(g.s., $J^\pi$ = 3/2$^-$; $E^*$= 0.429 MeV, $J^\pi$ = 1/2$^-$) + $d$ — $\alpha$−transfer. All states of the subsystems ii) and iii) are coupled with the subsystem i) by the reactions with protons and $\alpha$-particles transfers. Couplings between ground and excited states of nuclei $^6$Li and $^7$Be were calculated using the rotational model with the form factor $V_\lambda(r) = (\delta_\lambda / \sqrt{4\pi})dU(r)/dr$ for quadrupole transitions ($\lambda$ = 2). Here, $\delta_\lambda$ is a deformation length, which is determined by $\delta_\lambda = \beta_\lambda R$, where $R$ and $\beta_\lambda$ are the radius of the nucleus and the deformation parameter, respectively. The reorientation effects, determined by the matrix element $< E, J^\pi|V_2|E, J^\pi >$ [51], were also included in the coupling scheme. The deformation lengths $\delta_2$ were taken equal to 3.0 fm for $^6$Li, and 2.0 for $^7$Be, which correspond to $\beta_2 = 0.73$ and $\beta_2 = 1.0$, respectively [50, 52, 53].

The spectroscopic factors for the $^3$He and $^6$Li nuclei in the ($d+p$) and ($\alpha+d$) configurations, respectively, are fixed using the corresponding ANC values mentioned above. They are found to be 1.16 and 0.94, respectively. Whereas, the spectroscopic amplitudes for the $^7$Be nucleus in the ($^6$Li + $p$) and ($\alpha$ + $^3$He) configurations are taken from [54]. Nevertheless, the ratio of the DCSs calculated with and without the CCE contribution (defining the CCE renormalization factor for the ANCs from Eq. (1), calculated for each scattering angle belonging to the main peak of the angular distributions, as done in [50]), does not depend on these spectroscopic factors.

The values of the geometric parameters of the Woods-Saxon potential, used to calculate the two-body bound state wave functions, were taken as in [52]. For the $d - ^6$Li and $d - ^3$He core-core interactions in the proton transfer and $\alpha$-particle exchange mechanisms, the optical potentials adopted for the entrance ($^6$Li + $^3$He) channel and the Coulomb component for the $d - ^3$He potential were used, respectively.

The CCE contribution enhances the ANC values from 22% to 47% and up to 10.9% for $^3$He + $\alpha \to ^7$Be(g.s) and $^3$He + $\alpha \to ^7$Be(0.429 MeV), respectively, with respect to the DWBA calculation, and from 1.0% to 6.0% and from 1.6% to 12% for $^6$Li + $p \to ^7$Be(g.s.) and $^6$Li + $p \to ^7$Be(0.429 MeV), respectively. In particular,



Figure 3. Angular distributions of the $^6$Li($^3$He, $d$)$^7$Be reaction populating the ground (($a$) and ($c$)) and first (0.429 MeV) excited (($b$) and ($d$)) states of $^7$Be at the projectile $^3$He energies of 3 (($a$) and ($b$)) and 5 (($c$) and ($d$)) MeV. Error bars are smaller than the size of the points. Gray lines are the calculated angular distributions as described in the text, for $p$− and $\alpha$−transfer (forward and backward hemisphere, respectively).

the ranges of 1.13≤ $r_0$ ≤1.40 fm and 0.59≤ $a$ ≤0.72 fm and the depth of the potential well was adjusted to fit the corresponding experimental binding energy for each ($r_0$, $a$) pair.

To test the peripheral nature of the reaction, the geometrical parameters $r_0$ and $a$ of the Woods-Saxon potential of the bound state wave function were varied within the ranges as above (similarly to [50]) and the resulting $R^{(DWBA)}_{p; j_{6_{Li}p}}$ and $R^{(DWBA)}_{\alpha; j_{3_{He}\alpha}}$ functions were found to change within about ±7% at varying the ($r_0, \alpha$) pair in the intervals above, for each chosen experimental point of center-of-mass scattering angle $\theta$. By normalizing the calculated DCSs to the experimental ones for each experimental point ($\theta = \theta^{exp}$) separately for the forward and backward angle regions, the "indirectly determined" values of the ANCs for $^3$He + $\alpha \to ^7$Be and for $^6$Li + $p \to ^7$Be without and with taking into account the channels coupling effects (CCE) were derived.

The CCE contributions to the DWBA cross sec-

Fig. 3 shows the calculated DCSs, normalized to the corresponding main peak of the angular distributions at $\theta = \theta_{peak}^{exp}$, compared to the experimental results. For each experimental angular distribution, labelled from (a) to (d), two curves are shown, for the forward and the backward angles, corresponding to $p-$ and $\alpha-$particle transfer, respectively.

The weighed mean values of the square of the ANCs for the $^3$He $+ \alpha \rightarrow {}^7$Be(g.s.) and $^3$He $+ \alpha \rightarrow {}^7$Be(0.429 MeV) are equal to $C^2 = 20.84 \pm 1.12$ [0.82; 0.77] fm$^{-1}$ and $C^2 = 12.86 \pm 0.50$ [0.35; 0.36] fm$^{-1}$, respectively, which are in an excellent agreement with those of [24] derived from the analysis of the experimental $S-$factor data of [11, 13, 15, 16]. The overall uncertainties given here correspond to the errors combined in quadrature, including both experimental uncertainties in the $d\sigma^{exp}/d\Omega$ (first term in square parentheses) and the uncertainty corresponding to the ANC for $d + {}^4He \rightarrow {}^6$Li, as well as the uncertainties characterizing the $R_{\alpha; j_{3_{He\alpha}}}^{(DWBA)}$ function (second term in square parentheses).

## 4. Summary

The direct capture contribution to the astrophysically important $^3$He($^4$He,$\gamma$)$^7$Be reaction cross section at energies corresponding to the core temperature of the Sun was derived using the ANC technique. The angular distributions of deuterons emitted in the $^6$Li($^3$He,$d$)$^7$Be $\alpha$-transfer reaction were measured with high precision at $E_{^3He} = 3.0$ MeV and $E_{^3He} = 5.0$ MeV and the weighed means of the ANCs were used to calculate the total astrophysical $S-$factor at stellar energies (including $E = 0$). The calculations were performed within the modified two-body potential approach framework [46, 55], and the resulting $S_{34}(0)$ and $S_{34}(23$ keV) factors were found to be $S_{34}(0) = 0.534 \pm 0.025$ [0.015; 0.019] keVb and $S_{34}(23$ keV) $= 0.525 \pm 0.022$ [0.016; 0.016] keVb.

While the ANC approach is well established since decades (as discussed in the recent review [59]), additional work is necessary to address specific issues and improve the accuracy of the present paper. Among others, the uncertainty introduced by the use of one-step process in modelling the transfer, the couplings between ground and excited states of $^6$Li and $^7$Be, and the need of coupled-channel analysis to derive the $^3$He+$^4$He and the $p + {}^6$Li ANCs. The present result provides a completely independent confirmation of the cross section-based extrapolation of [14, 24, 29], and the deduced ANCs for the $p + {}^6$Li system further support the present result. Moreover, the indirectly derived ANC values can also be used in future R-matrix extrapolations to increase the precision and the reliability, since they supply additional constraints on the R-matrix analysis [58].

## References

[1] E. G. Adelberger *et al.*, Rev. Mod. Phys. **70**, 1265 (1998).
[2] E. G. Adelberger *et al.*, Rev. Mod. Phys. **83**, 195 (2011).
[3] R. H. Cyburt, and B. Davids, Phys. Rev. C **78**, 064614 (2008).
[4] R. G. Pizzone et al., Astrophys. J. **786**, 112 (2014).
[5] The Borexino Collaboration, Nature, **562**, 505 (2018).
[6] B. Aharmim *et al.*, (SNO Collaboration), Phys. Rev. C **81**, 055504 (2010).
[7] K. Abe *et al.*, (Super-Kamiokande Collaboration), Phys. Rev. D **83** 052010 (2011).
[8] N. Vinyoles *et al.*, Astrophys. J. **852**, 202 (2017).
[9] W. C. Haxton, and A. M. Serenelli, Astrophys. J. **687**, 678 (2008).
[10] J. N. Bahcall, and M. H. Pinsonneault, Phys. Rev. Lett. **92**, 121301 (2004).
[11] D. Bemmerer *et al.*, Phys. Rev. Lett. **97**, 122502 (2006).
[12] T. A. D. Brown, C. Bordeanu, K. A. Snover, D. W. Storm, D. Melconian, A. L. Sallaska, S. K. L. Sjue, and S. Triambak, Phys. Rev. C. **76**, 055801 (2007).
[13] F. Confortola, *et al.*, Phys. Rev. C **75**, 065803 (2007).
[14] A. Kontos, E. Uberseder, R. deBoer, J. Görres, A. Akers, A. Best, M. Couder, and M. Wiescher, Phys. Rev. C **87**, 065804 (2013).
[15] B. S. Nara Singh, M. Hass, Y. Nir-El, and G. Haquin Phys. Rev. Lett. **93**, 262503 (2004).
[16] Gy. Gyürky *et al.*, Phys. Rev. C **75**, 035805 (2007).
[17] M. Carmona-Gallardo *et al.*, Phys. Rev. C **86**, 032801(R) (2012).
[18] C. Bordeanu, Gy. Gyürky, Z. Halász, T. Szücs, G. G. Kiss, Z. Elekes, J. Farkas, Zs. Fülöp, and E. Somorjai E. Nucl. Phys. A **908**, 1 (2013).
[19] T. Szücs, G. G. Kiss, Gy. Gyürky, Z. Halász, T. N. Szegedi, and Zs. Fülöp, Phys. Rev. C **99**, 055804 (2019).
[20] Di Leva *et al.*, Phys. Rev. Lett. **102**, 232502 (2009).
[21] T. A. Tombrello, and P.D. Parker, Phys. Rev. **131**, 2582 (1963).

[22] P. Mohr, H. Abele, R. Zwiebel, G. Staudt, H. Krauss, H. Ober-hummer, A. Denker, J. W. Hammer, G. Wolf, Phys. Rev. C **48**, 1420 (1993).
[23] P. Mohr, Phys. Rev. C **79**, 065804 (2009)
[24] Q. I. Tursunmahatov, and R. Yarmukhamedov, Phys. Rev. C **85**, 045807 (2012).
[25] T. Kajino, H. Toki, and S. M. Austin, Astrophys. J. **319**, 531 (1987).
[26] T. Neff, Phys. Rev. Lett. **106**, 042502 (2011).
[27] K. M. Nollett, Phys. Rev. C **63**, 054002 (2001).
[28] P. Descouvemont, A. Adahchour, C. Angulo, A. Coc, and E. Vangioni-Flam, At. Data Nucl. Data Tables **88**, 203 (2004).
[29] R. J. deBoer, J. Görres, K. Smith, E. Uberseder, M. Wiescher, A. Kontos, G. Imbriani, A. Di Leva, and F. Strieder, Phys. Rev. C **90**, 035804 (2014).
[30] T. Kajino, Nucl. Phys. A **460**, 559 (1986).
[31] J. Dohet-Eraly, P. Navrátil, S. Quaglioni, W. Horiuchi, G. Hupin, and F. Raimondi, Phys. Lett. B **757**, 430 (2016).
[32] X. Zhang, K. Nollett and D. R. Philips, J. Phys. G accepted for publication (https://iopscience.iop.org/article/10.1088/1361-6471/ab6a71)
[33] A. M. Mukhamedzhanov *et al.* Phys. Rev. C **63** 024612 (2001).
[34] H. M. Xu, C. A. Gagliardi, R. E. Tribble, A. M. Mukhamedzhanov, and N. K. Timofeyuk, Phys. Rev. Lett., 73 (1994) 2027
[35] A. M. Mukhamedzhanov *et al.*, Phys. Rev. C **67**, 065804 (2003).
[36] J. P. Schiffer, T. W. Bonner, R. H. Davis, and Jr. F. W. Prosser, Phys. Rev. **104**, 1064 (1956).
[37] H. G. Bingham, A. R. Zander, K. W. Kemper, and N. R. Fletcher, Nucl. Phys. A **173**, 265 (1970).
[38] E. D. Johnson *et al.*, Phys. Rev. Lett **97**, 192701 (2006).
[39] E. D. Johnson, G. V. Rogachev, J. Mitchell, L. Miller and K. W. Kemper, Phys. Rev. C **80**, 045805 (2007).
[40] A.M.Mukhamedzhanov *et al.*, Phys. Rev. C **56**, 1302 (1997).
[41] E.I. Dolinsky *et al.*, Nucl. Phys. **202**, 97 (1973).
[42] R.M. DeVries, Ph.D. thesis, Ubiversity of California, 1971; J. Perrenoud and R.M. DeVries, Phys.Lett.B **36**, 18 (1971).
[43] L.D. Blokhintsev *et al.*, Fiz. Elem. Chastits At. Yadra. **8**, 1189 (1977)[Sov. J. Part. Nucl. **8**, 485 (1977)].
[44] E.A. George and L.D. Knutson, Phys. Rev. C **59**, 958 (1999).
[45] R. Yarmukhamedov and L.D. Blokhinstev, Phys. At. Nucl., **81**, 616 (2018).
[46] K.I. Tursunmakhtov and R. Yarmukhamedov, IJMP:Conf.Series, **49**, 1960017 (2019).
[47] S.V. Artemov *et al.*, Yad. Fiz. **59**, 454 (1996)[Phys. Atom. Nucl. **59** , 428 (1996)].
[48] H. Ludecke *et al.*, Nucl. Phys. A **109**, 676 (1968).
[49] M. Avrigeanu *et al.*, Nucl. Phys. A **759**, 327 (2005).
[50] O. Tojiboev *et al.*, Phys. Rev. C **94**, 054616 (2016).
[51] I.J. Thompson, Comput. Phys. Rep. **7**, 167 (1988); I.J. Thompson FRESCO, Department of Physics, University of Surrey, July 2006, Guildford GU2 7XH, England, version FRESCO 2.0, http://www.fresco.org.uk/.
[52] N. Burtebayev *et al.*, Nucl. Phys. A **909**, 20 (2013).
[53] N. Burtebayev *et al.*, Yad. Fiz. **59**, 33 (1996) [Phys. Atom. Nucl. 59, 29 (1996).
[54] O.F. Nemets *et al.*, Nucleons Associations in Atomic Nuclei and Multi-nucleon Transfer Reactions (in Russian), Naukova Dumka, Kiev, 1988.
[55] S. B. Igamov and R. Yarmukhamedov, Nucl. Phys. A 781, 247 (2007); 832, 346 (2010).
[56] M, P. Takács *et al.*, Phys. Rev. D **91**, 123526 (2015).
[57] M.P. Takács *at al.*, Nucl. Phys. A **970**, 78 (2018)
[58] A.M. Mukhamedzhanov *et al.*, Phys. Rev. C **78**, 015804 (2008).
[59] R.E. Tribble *et al.*, Rep. Prog. Phys. **77**, 106901 (2014)

## 6. Appendix A

In table 1 we show the the squared ANCs and their uncertainties ($C_\alpha^2$) for the $\alpha + {}^3\text{He} \rightarrow {}^7\text{Be}$ system, obtained in the present work without and with the CCE contributions, for each experimental point of center-of-mass angle $\theta$, at $E_{{}^3\text{He}} = 3.0$ and $5.0$ MeV, and their weighed mean values, for both ${}^7\text{Be}$ ground state ($E^* = 0.0$ MeV; $J^\pi = \frac{3}{2}^-$) and first excited state ($E^* = 0.429$ MeV; $J^\pi = \frac{1}{2}^-$).

The numbers in square brackets are the experimental ($\Delta C_{\text{exp}}^2$) and theoretical ($\Delta C_{\text{th}}^2$) uncertainties, respectively. They are calculated as follows: the experimental uncertainty is the sum of two contributions, $\Delta_{\text{exp}}^{(\text{tot})} = [(\Delta_{\text{exp}}^{(1)})^2 + (\Delta_{\text{exp}}^{(2)})^2]^{1/2}$, first one being the uncertainty on the experimental angular distributions: $\Delta_{\text{exp}}^{(1)} = [\Delta(d\sigma^{\text{exp}}/d\Omega)]/[d\sigma^{\text{exp}}/d\Omega]$, and the second one is linked to the uncertainty on the $\alpha + d \rightarrow {}^6\text{Li}$ ANC: $\Delta_{\text{exp}}^{(2)} = \Delta(C^{\text{exp}})^2/(C^{\text{exp}})^2$. The theoretical uncertainty, corresponding to the effects of the non-peripherality, is calculated from the $R$-functions 2: $\Delta_{\text{th}} = \Delta R^{\text{DWBA}}/R^{\text{DWBA}}$ (for ease of reading, all subscripts are neglected here). In detail, the uncertainty on the $R$-function is calculated varying the geometrical parameters ($r_0$ and $a$) of the adopted Woods-Saxon potential within the intervals mentioned in the text. Finally, the total error is calculated taking the square root of the experimental and theoretical uncertainties summed in quadrature: $\Delta_{\text{tot}} = [(\Delta_{\text{exp}}^{(\text{tot})})^2 + (\Delta_{\text{th}})^2]^{1/2}$.

Table 1. Summary of all uncertainties entering the evaluation of the ANC of the $\alpha + {}^3\text{He} \to {}^7\text{Be}$ system. More detail are given in Appendix A.

| $E_{{}^3\text{He}}$ [MeV] | $E^*$ [MeV] | $\theta$ [deg] | $\alpha + {}^3\text{He} \to {}^7\text{Be}$ $C_\alpha^2$ [fm$^{-1}$] without CCE | with CCE | $\Delta_{\text{exp}}^{(1)}$ % | $\Delta_{\text{exp}}^{(2)}$ % | $\Delta_{\text{exp}}$ % | $\Delta_{\text{th}}$ % | $\Delta_{\text{tot}}$ % |
|---|---|---|---|---|---|---|---|---|---|
| 1 | 2 | 3 | 4 | 5 | 6 | 7 | 8 | 9 | 10 |
| 3.0 | 0.0 | 158.4 | 14.66±1.57[1.18;1.03] | 17.87±1.91[1.44;1.25] | 4.3 | 6.8 | 8.0 | 7.0 | 10.7 |
|  |  | 162.0 | 17.36±1.85[1.39;1.22] | 21.49±2.29[1.72;1.50] | 4.2 | 6.8 | 8.0 | 7.0 | 10.6 |
|  |  | 164.9 | 17.68±1.91[1.46;1.24] | 22.17±2.40[1.83;1.55] | 4.6 | 6.8 | 8.0 | 7.0 | 10.8 |
| 5.0 |  | 154.7 | 14.99±1.57[1.17;1.05] | 20.40±2.14[1.59;1.43] | 3.8 | 6.8 | 7.8 | 7.0 | 10.5 |
|  |  | 158.1 | 14.69±1.55[1.16;1.03] | 21.63±2.29[1.71;1.51] | 4.2 | 6.8 | 7.9 | 7.0 | 10.6 |
|  |  | 161.7 | 15.88±1.59[1.14;1.11] | 23.03±2.31[1.65;1.61] | 2.2 | 6.8 | 7.2 | 7.0 | 10.0 |
| 3.0 | 0.429 | 160.0 | 10.71±1.10[0.80;0.75] | 11.60±1.19[0.87;0.81] | 3.2 | 6.8 | 7.5 | 7.0 | 10.2 |
|  |  | 163.3 | 11.67±1.20[0.88;0.82] | 12.70±1.31[0.96;0.89] | 3.2 | 6.8 | 7.5 | 7.0 | 10.3 |
|  |  | 166.3 | 10.81±1.25[0.83;0.76] | 11.83±1.23[0.91;0.83] | 3.6 | 6.8 | 7.5 | 7.0 | 10.4 |
|  |  | 169.4 | 12.61±1.32[0.98;0.88] | 13.90±1.45[1.08;0.97] | 3.7 | 6.8 | 7.7 | 7.0 | 10.4 |
|  |  | 172.5 | 12.31±1.26[0.92;0.86] | 13.65±1.40[1.02;0.96] | 3.1 | 6.8 | 7.5 | 7.0 | 10.2 |
| 5.0 |  | 155.6 | 13.80±1.56[1.22;0.97] | 12.86±1.45[1.14;0.90] | 5.7 | 6.8 | 8.9 | 7.0 | 11.3 |
|  |  | 158.9 | 13.34±1.39[1.06;0.90] | 12.87±1.34[1.02;0.90] | 4.0 | 6.8 | 7.9 | 6.8 | 10.4 |
|  |  | 162.0 | 13.74±1.39[1.00;0.96] | 13.72±1.39[1.00;0.96] | 2.6 | 6.8 | 7.3 | 7.0 | 10.1 |
|  |  | 165.4 | 13.32±1.46[1.12;0.93] | 13.74±1.51[1.16;0.96] | 5.0 | 6.8 | 8.4 | 7.0 | 11.0 |
|  |  | 168.5 | 14.73±1.84[1.32;1.03] | 15.69±1.96[1.40;1.10] | 5.8 | 6.8 | 9.0 | 7.0 | 12.5 |
|  |  |  | the weighted mean value | | | | | | |
| 3.0+5.0 | 0.0 |  | 15.68±0.74[0.51;0.53] | 20.84±1.12[0.82;0.77] |  |  | 3.9 | 3.7 | 5.4 |
| 3.0 |  |  | 16.32±1.41[1.00;1.00] | 20.13±1.97[1.39;1.39] |  |  | 6.9 | 6.9 | 9.8 |
| 5.0 |  |  | 15.18±0.91[0.67;0.61] | 21.66±1.10[0.95;0.87] |  |  | 4.3 | 4.0 | 5.0 |
| 3.0+5.0 | 0.429 |  | 12.12±0.62[0.43;0.44] | 12.86±0.50[0.35;0.36] |  |  | 2.7 | 2.8 | 3.9 |
| 3.0 |  |  | 10.84±0.60[0.36;0.36] | 11.80±0.62[0.44;0.44] |  |  | 3.7 | 3.7 | 5.2 |
| 5.0 |  |  | 13.74±0.66[0.50;0.43] | 13.62±0.69[0.50;0.48] |  |  | 3.7 | 3.5 | 5.1 |